One-probe nanoprobing of power devices and electronic packages

Chengliang Huang[1], Vignesh Viswanathan[2], Andreas Rummel[3], Greg M. Johnson[4], Heiko Stegmann[4], Elliott Andrew[5], Allen Gu[4], Masako Terada[4], Thomas Rodgers[4]

[1] Carl Zeiss Co. Ltd, Shanghai, China
[2] Carl Zeiss Pte Ltd, Singapore
[3] Kleindiek Nanotechnik, Ruetlingen, Germany
[4] Carl Zeiss Microscopy GmbH, Oberkocken, Germany
[5] Carl Zeiss Limited, Cambridge, United Kingdom

Abstract— **Results involving the use of a single nanoprobing contact are presented, on both a SiC planar MOSFET device, and a small system-in package. In both cases, mechanical polished samples were prepared, and then probed with a single contact. For the SiC MOSFET, the depletion zones were imaged while the samples were mounted on a 45 ° stub. Discussion of the different signals generated from Passive Voltage Contrast (PVC) and Electron Beam Induced Current (EBIC), as well as possible artifacts of sample grounding, are provided. For the package, Electron Beam Absorbed Current (EBAC) provided indication of connected features within the sample. The experiment showed the capability of measuring features across three orders of magnitude in size.**

Keywords—EBAC, EBIC, package, SiC, nanoprobing, PVC

I. Introduction

A semiconductor failure analysis lab may have to work with a wide variety of failure types and form factors, especially if that were one working with packaging. That is because a failure may occur anywhere from the relatively large-scale wiring of the package to intricate devices or transistors deep inside the chip. For this work, two types of form factors were considered for study, a planar SiC MOSFET, and a system in package.

Power semiconductors are increasingly important to a wide range of industrial applications. SiC valued for its low resistance and high breakdown voltage. Thus, it is seeing increasing applications [1] in power conversion, elevators, [2], and in the drivetrain and charging systems of electric vehicles. [3] As such, SiC devices may suffer from a number of failure modes, including those such as body diode degradation [4], or involve hot carriers in the depletion zone. [5] [6] . Because these properties will depend on the health of the *p/n* junctions in a sample, techniques which enable the evaluation of junction health and placement will be of great interest in yield monitoring and failure analysis.

At the same time, on a much larger scale, packaging FA is becoming more challenging. Concepts like Heterogeneous Integration (HI) [7] will introduce complexities in layers, stacking, materials, etc. which will only make it more important to be able to perform localization on as large and as intact a sample as possible. For this experiment, the ADAQ23875 µModule® Data Acquisition Solution is a System-in-Package was used as a model test vehicle for the evaluation of the technique, with the use of a randomly selected, good device.

II. Techniques

A. Electron Beam Induced Current and Passive Voltage Contrast

Two techniques are available for the examination of p/n junctions, EBIC [8] and PVC [9]. The theoretical backgrounds for these two are discernable by consulting the energy band diagram for a p/n junction, as shown in Figure 1. The most simple technique that most engineers would have exposure to in electron microscopy is passive voltage contrast, which will often occur naturally due to different properties within the area examined. Across the p/n junction there is a difference in electron affinity, as depicted by the sloping shape of the conduction band of the junction. As the sample is scanned with an electron beam, any electrons seeking to escape from the N side will incur an energy penalty relative to the P side. Thus, there will be a lower secondary electron yield, and a lower energy among those electrons that do escape. Detection of such secondary electron energy distributions would require an electron microscope sensitive to low-energy secondary electrons [10]. It should be noted that the PVC effect is constant across the entire implant region.

The second technique, also informed by Figure 2, is Electron Beam Induced Current for evaluation of *p/n* junctions has been widely studied [11] [8] [12] [13] . Here, any charge that is introduced to a region with sloped energy profiles—the depletion region—will see an electric field that will push the carriers, and this movement of carriers may be detected as a current if a probe is opportunistically placed on the sample. These carriers may be due to the incident electron beam, secondary electrons, or any electron-hole pairs created by the beam. It should be noted that this effect only occurs at the depletion zone. Charge introduced at other places is either recombined or lost to ground.

A third probing technique is Electron Beam Absorbed Current, which simply maps regions of connectivity in the sample. The probe acts as either a path to ground for the electrons impinging upon the sample, or re-supplies electrons lost due to secondary electron emission in the sample.

These two techniques in this system were conducted by use of a Kleindiek MM3E prober and amplification system, and imaging in a SigmaSEM 300.

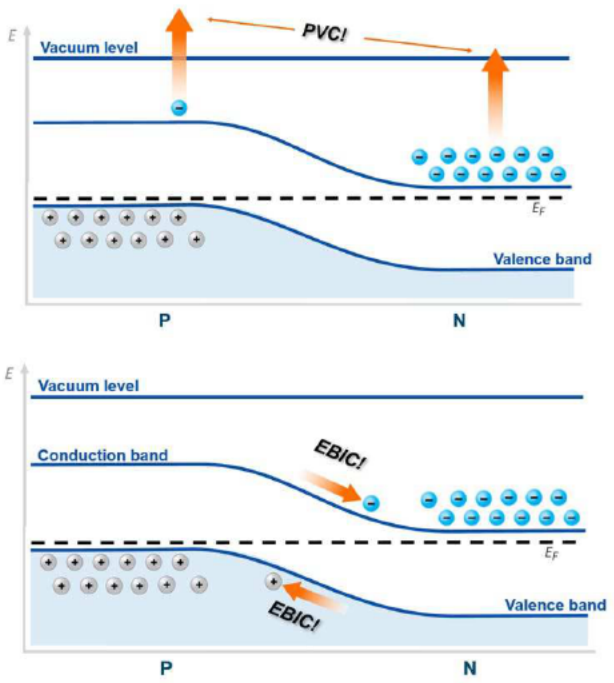

Figure 1. Band diagram for a p/n junction, indicating how these electrical properties influence microscopy techniques at operate on junctions. The top image explains how the P and N sides of a junction have a different electron affinity, and this imposes an energy penalty on any secondary electrons that might want to escape the N side. The depicts how the electric field at a p/n junction's depletion zone will cause EBIC currents at the junction, and not over the full body of the device.

III. PROCEDURE

A. *Sample selection and preparation*

For the first section, a commercially available SiC MOSFET chip was selected, and a mechanically polished cross section was prepared, perpendicular to the gates. The samples were attached by carbon tape to 45-degree stubs which were placed in a 9-stub carousel. The microprobes then came in from a roof mounting to approach and touch down on the samples The samples were then inserted in a Sigma 300 ZEISS SEM. The EBIC analysis was performed with a MM3A nanoprobing system provided by Kleindiek Nanotechnik. Several other samples were also mounted similarly on a 9-up carousel and examined at the same time. The setup is depicted in Figure 2, as seen from the chamberscope of the SEM.

Other samples were cleaved and examined at 90 ° in a GeminiSEM 300.

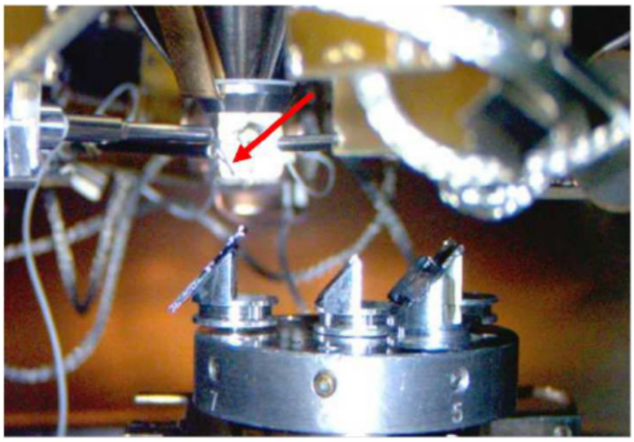

Figure 2. Chamber scope view of the experimental setup for the study. Several polished cross sections of chips were mounted on 45° stubs and placed on the same carousel. The probe needle is raised above the sample and is just visible at the red arrow

For the second section, a commercially available ADAQ23875 system-in-package (SiP) device was purchased using a standard commercial channel. The sample then was imaged by 3D X-ray microscopy in a Versa XRM system. at 10 µm/voxel resolution to capture full field of view (FOV) of the package. 120 kV X-ray energy was used to image this medium density sample. Then the package was mounted in epoxy inside a standard 2-inch metallographic mount, and polished with mechanical polishing and alumina slurry. The resulting "puck" was then examined with a GeminiSEM 300. A depiction of this setup is shown in the optical photo of Figure 3.

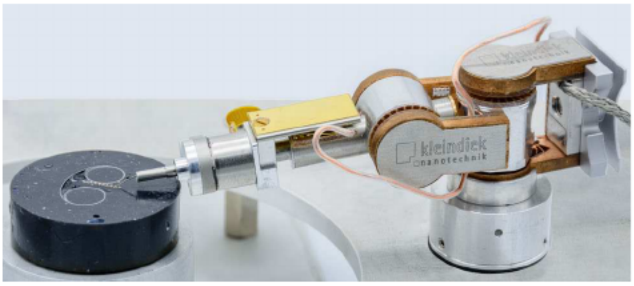

Figure 3. Demonstration of the placement of a nanoprobing probe on a polished cross section (optical photo, outside of chamber).

IV. RESULTS

A. *SiC MOSFET*

Figure 4 depicts the SiC MOSFET used in this analysis. The cartoon on the left depicts the typical implant regions used in the top half of the chip, and the image at right is from the cleaved surface. One can easily see the implant regions of the N+ source, P-well, and the N regions below.

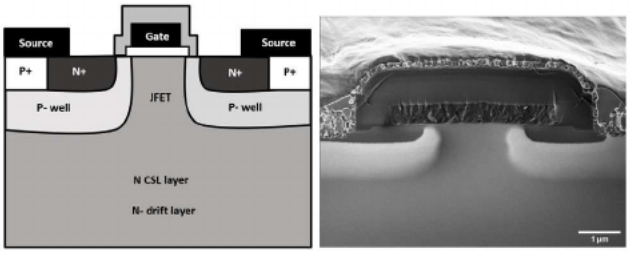

Figure 4. Diagram and cross-sectional image of the implant regions around a gate in a SiC MOSFET. Left: cartoon of implant regions and names (not to scale). Right: 2 kV Inlens image of device from the same area.

Figure 5 now compares the same general view of two different chips: the polished section, viewed on a 45° stub, with 60 um aperture, and the image from Figure 2 taken with a lower aperture, on a cleaved surface, at 90°. The greater current and angle provide for more sensitivity [14] in some voltage contrast, such that we can now distinguish (left image) among the N-doped regions of the JFET, CSL layer, and N-drift regions.

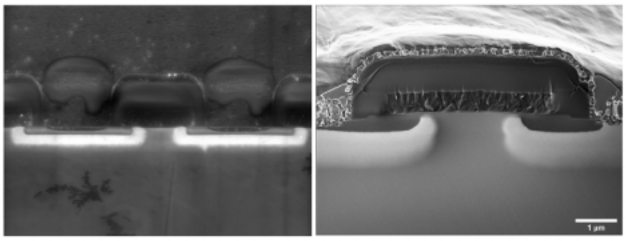

Figure 5. Diagram and cross-sectional image of the implant regions around a gate in a SiC MOSFET. Left: cartoon of implant regions and names (not to scale). Right: 2 kV Inlens image of device from the same area.

For the next set of experiments, with a 60 µm aperture, EBIC images were taken from the cleave, as shown in Figure 6, at three different beam acceleration potentials. In all images, one can see a small white zone beneath the main EBIC signal. It is believed that these may be an artifact of the degree of grounding possible with the use of a single probe. It is also clear that as the beam energy gets above 5 kV, the electron scattering cloud becomes unusually large, and therefore one is sampling from too large an area to get a meaningful characterization of the depletion zone.

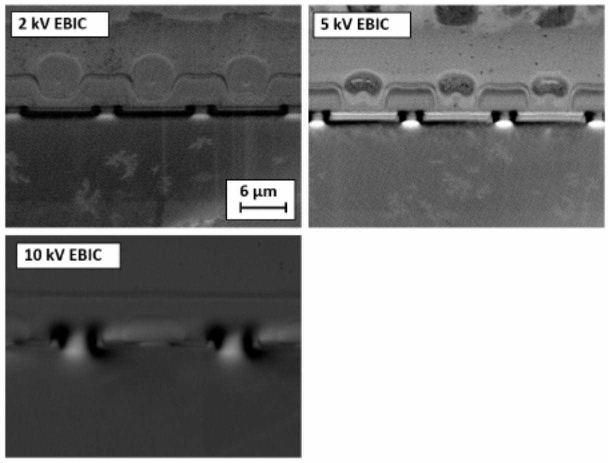

Figure 6. EBIC images at 2 kV, 5 kV, and 10 kV for the devices

Next the PVC and EBIC images were compared side by side, as seen in Figure 7. It is clear that these zones highlight different features in the p/n junctions.

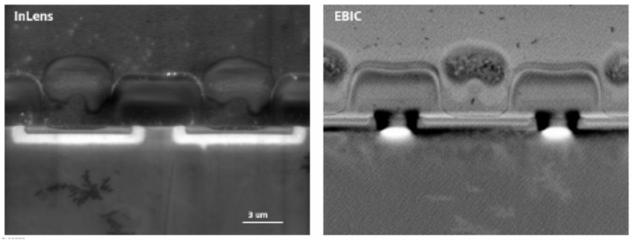

Figure 7. InLens and 5 kV EBIC images generated from the SiC MOSFET. In the InLens image, the P- well region stands out in bright contrast against the surrounding N-type regions, due to PVC. In the EBIC images, the depletion zone between this P-well and surrounding N- drift regions is highlighted in black. An additional white spot is seen, which may be a combination of the grounding problem introduced by use of a single probe, and the resistance at the JFET region of the device.

B. ADAQ23875 section

Three views of the System-in-Package sample are shown in Figure 8. At left is a light microscopy image. In the middle and right, respectively, are two different virtual reconstructions from XRM data of the top and middle planes in the sample. From the 3D reconstruction is it possible to examine multiple planes in the sample, choose a feature of interest, and as desired, to note top surface features that will enable one to target for section and thus find buried features underneath.

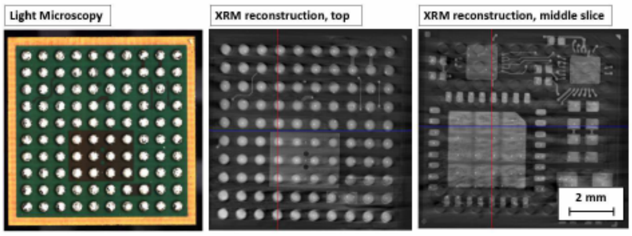

Figure 8. Multiple views of the ADAQ23875 package, including optical, and two different reconstructions from XRM data, taken at different virtual slices in the sample.

Next the polished cross section of the package was examined in SEM. It is seen in Figure 9.

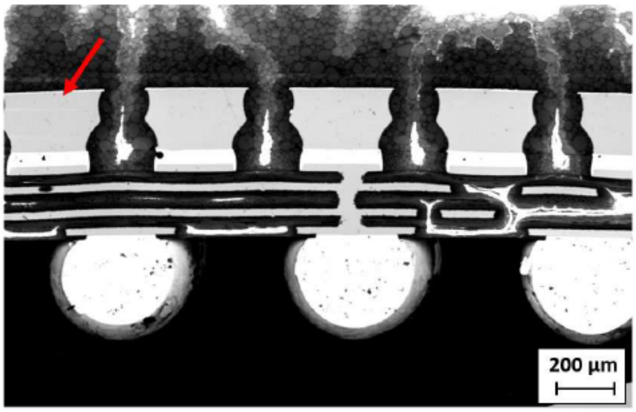

Figure 9. SEM micrograph at 15 kV of a random, polished, mechanical cross section of the package. The feature tested for continuity is at the left in the image.

Figure 10 shows the EBAC results undertaken at 20 kV. Only a single metal feature is highlighted, indicating that the section has intersected a feature that was disconnected from its net by the plane of section. It nevertheless demonstrates the utility of the technique.

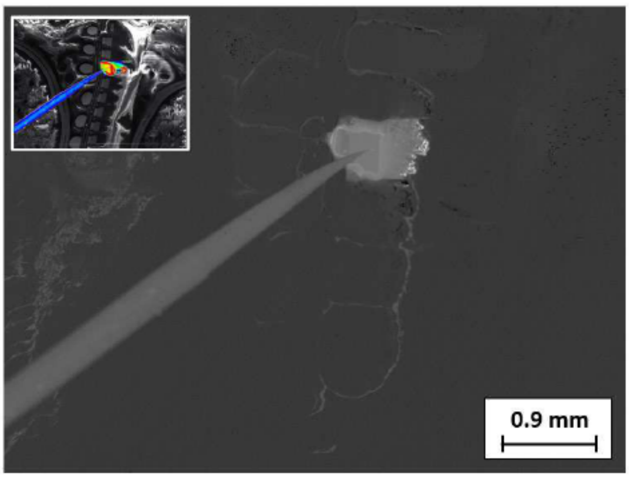

Figure 10. Results from nanoprobing a specific metallic feature in the polished cross section. Inset: 20 kV SEM image with color overlay of the EBAC signal. Main image: EBAC image showing the one feature and that there are no features next to it, indicating that the cross section has cut off this wire from its surroundings.

V. SUMMARY

Results were presented from two different types of analysis, showing nanoprobing characterization of sections of either a power device or a package. In the SiC MOSFET, the depletion zones of the sample were clearly imaged, as well as clear PVC images of the implant regions. It is likely one spurious feature was seen that may be due to the degree of grounding possible with a single probe.

For the System-in-Package, XRM data was combined with a cross section to demonstrate the ability to probe one net in a sample.

VI. CONCLUSIONS

This study has shown that nanoprobing with a single, manipulatable probe offers versatility in everything from EBIC of p/n junctions, to accommodating a large polished structure. Effective results across three orders of magnitude in magnification.

A sample preparation workflow is shown for examination of p/n junctions. These results show useful properties of the junction even in cases where there may be some debris on the surface. Multiple samples can be examined each within a five minute window.

The work demonstrates what passive voltage contrast can do. It highlights levels of N-doping between the JFET, CSL, and N- drift region.

By virtue of being on 45 degree mounted samples, the work demonstrates the fundamental difference between EBIC and PVC. PVC is fundamentally a surface effect, related to the energy penalty that escaping secondary electrons undergo between differently doped regions, those with different electron affinities. EBIC meanwhile is more of a volume sampling effect, related to the introduction of charge into a region, which naturally spreads into the sample according to Monte Carlo physics into a teardrop-shaped bulb. In this experiment, higher kV was particularly unhelpful in that it was likely that the bulb was so large as to sample from regions of different implant regions.

The work also showed that grounding is key to eliminating artifacts that may influence the interpretation of the background level.

This work also shows a workflow where one may use XRM to find a net in question, mount a sample on a 2 inch puck, polish to a net in question, based on top surface marks, and then use EBAC to trace nets on the surface of the sample.

For advanced logic nodes with, say, 20 nm features, one may want a more sophisticated system, but whether looking at a planar compound semiconductor or a package, these systems appear to work well for the application

It takes less than 5 mins to land one probe on the target sample structure. This setup is capable of quick and streamlined in-situ electrical chacterization in SEM.

VII. FUTURE WORK

These results have strong merit for the power devices examined, devices in for a future paper after further optimization of the technique.

VIII. REFERENCES

[1] V. Veliadis, "SiC chip cost, the impact of defects and the case of price parity with Si at the system level," SEMI webinar series, June 6, 2023.

[2] T. Kimoto, "SiC Power Devices: Overview, Defect Electronics, and Reliability," in *IRPS Tutorial*, 2019.

[3] J. Palmour and J. Edmond, "The golden age of silicon carbide: 25 years of innovation," *Compound Semiconductor,* no. 6, pp. 38-42, 2020.

[4] B. J. Nel and S. Perinpanayagam, "A brief overview of SiC MOSFET failure modes and design reliability," in *The 5th International Conference on Through-life Engineering Services*, 2017.

[5] B. Kok, M. Looi and H. Goh, " Insulated Gate Bipolar Transistor Failure Analysis in Overvoltage Condition," in *ICREPQ'12*.

[6] N. Valentine, D. Das and M. M. Pecht, "Failure Mechanisms of Insulated Gate Bipolar Transistors (IGBTs)," in *2015 NREL Photovoltaic Reliability Workshop*.

[7] G. Kenyon, "Heterogeneous Integration and the evoluation of IC packaging," EE Times Europe, 6 April 2021.

[8] J. R. Beall and L. C. Hamiter, "EBIC - A Valuable Tool for Semiconductor Evaluation and Failure Analysis.," *15th International Reliability Physics Symposium,* pp. 61-69, 1977.

[9] R. Rosenkranz, ""Failure localization with active and passive voltage contrast in FIB and SEM"," *Journal of Materials Science-materials in Electronics,* 2011.

[10] J. Jatzkowski, M. Simon-Najasek and F. Altmann, "Novel techniques for dopant contrast analysis on real IC structures," *Microelectronics Reliability,* 2012.

[11] E. Cole, ""Beam-Based Defect Localization Techniques"," *ISTFA,* vol. Tutorials, 2007.

[12] K. Nikawa, "Method and system for testing an interconnection in a semiconductor integrated circuit," *US Patent number 5,804,980.*

[13] A. Rummel, G. Johnson and M. Kemmler, "Low-voltage EBIC investigation of EBIC fails," *IPFA,* 2021.

[14] H. Seiler, "Secondary electron emission in the scanning electron microscope," *Journal of Applied Physics,* vol. 54, no. doi: 10.1063/1.332840, 1983.